AIAA 2001-1599

CRYOGENIC TANK STRUCTURE SIZING WITH STRUCTURAL OPTIMIZATION METHOD

J.T.Wang, T.F.Johnson, D.W.Sleight, and E.Saether
NASA Langley Research Center
Hampton, VA 23681

42nd AIAA/ASME/ASCE/AHS/ASC Structures, Structural Dynamics, and Materials Conference
April 16-19, 2001/Seattle, WA

CRYOGENIC TANK STRUCTURE SIZING WITH STRUCTURAL OPTIMIZATION METHOD

J. T. Wang, T. F. Johnson, D. W. Sleight, and E. Saether
NASA Langley Research Center
Hampton, VA

Abstract

Structural optimization methods in MSC /NASTRAN are used to size substructures and to reduce the weight of a composite sandwich cryogenic tank for future launch vehicles. Because the feasible design space of this problem is non-convex, many local minima are found. This non-convex problem is investigated in detail by conducting a series of analyses along a design line connecting two feasible designs. Strain constraint violations occur for some design points along the design line. Since MSC/NASTRAN uses gradient-based optimization procedures, it does not guarantee that the lowest weight design can be found. In this study, a simple procedure is introduced to create a new starting point based on design variable values from previous optimization analyses. Optimization analysis using this new starting point can produce a lower weight design. Detailed inputs for setting up the MSC/NASTRAN optimization analysis and final tank design results are presented in this paper. Approaches for obtaining further weight reductions are also discussed.

Introduction

The field of structural optimization is well developed and is increasingly used in automotive, aerospace, machine design, civil, and other engineering fields [1,2,3]. Structural optimization methods are useful for conducting trade-off studies and sizing of structures. Future launch vehicles must be highly reliable lightweight structures to achieve the goal of affordable space travel. Designers of future launch vehicles need to take full advantage of optimization methods to obtain lightweight vehicle designs and evaluate them for meeting high reliability design requirements.

In future launch vehicles, cryogenic tanks will not only carry liquid oxygen (LOX) and hydrogen (LH2) fuel, but also function as the primary vehicle load carrying members. Current designs of lifting body type launch vehicles use multi-lobed tank configurations [4]. Such designs require the use of external rib-like standoff structures to support thermal protection tiles over the lobed intersections to create smooth aerodynamic surfaces. A recent study at NASA Langley Research Center (LaRC) found that the fuel volume efficiency could be enhanced by developing a conformal tank that closely follows the outside mold line of the vehicle [4]. The LaRC's conformal cryogenic tank design and its dimensions are shown in Figure 1.

The objective of this study is to use the optimization capabilities available in MSC/NASTRAN [5] for sizing and weight reduction of honeycomb sandwich conformal cryogenic tank structures. The facesheet and honeycomb core thicknesses of the sandwich structures are used as design variables to be optimized. The NASTRAN input entries for optimizing these design variables are developed and tested. Technical difficulties encountered in using optimization for sizing and finding optimal low weight design of the conformal tank are discussed. Nonconvexity of the feasible design space, which can often have local minima, is investigated. A simple procedure for finding a better optimization starting point for converging to a lower weight design is introduced. Finally, a geometric nonlinear analysis is performed to confirm that the final design, obtained from linear optimization analyses, meets all the design constraints.

Design Requirements and Loads

All the tank structures are assumed to be symmetric sandwich constructions. One of the most important design requirements for the LOX or LH2 cryogenic tanks is that the minimum tank wall thickness can meet permeability constraints. For the sandwich tank wall, the minimum inner facesheet thickness is 0.06 in. and the strain allowable of the facesheet is 6,000 microstrain (6.0×10^{-3} in./in.). However, further analyses and experimental tests are required to validate this design requirement. The thickness of the outer facesheet is assumed to be equal to the inner facesheet to avoid coupling between bending and extension.

The design requirements and loading conditions used in this tank sizing and analysis study are based on data reported in the literature [4, 6]. The present study uses the most severe loading condition, which corresponds

to a 3-G axial acceleration. The characteristics of this loading condition are listed in Table 1.

Table 1. Maximum 3-G Axial Acceleration Load Condition.

Loading Description	Value
Velocity	4,140 ft/sec.
Angle-of-Attack	-0.044 degrees
Axial Thrust Force	4.36×10^6 lbs.
Axial Drag Force	-1.85×10^5 lbs.
Vehicle Acceleration	3.0 g's (Axial)
	0.063 g's (Normal)
Tank Ullage Pressure	25.0 psig (LOX)
	30.0 psig (LH2)
Fluid Weight	
LOX (46.2% full)	0.91×10^6 lbs.
LH2 (50.0% full)	0.164×10^6 lbs.

Material Properties

Material properties representing a quasi-isotropic lay-up of toughened graphite epoxy (IM7/977-2) tape material are used for sizing the tank structures. Material properties and minimum gage requirements are presented in Table 2.

Table 2. Material properties and minimum gages.

Property Description	Value
Quasi-Isotropic IM7/977-2 Laminate	
Young's Modulus (Msi)	8.804
Shear Modulus (Msi)	3.354
Poisson's Ratio	0.312
Density (lb./in.^{3})	0.057
Tank wall strain allowable (tension/compression, in./in.)	0.006
Minimum Gage* – Tanks (in.)	0.06
Minimum Gage* – Intertank (in.)	0.04
Minimum Gage* – Internal structures (in.)	0.02
Honeycomb Core (Phenolic, 3.0 lb./ft.^{3})	
Shear Modulus (ribbon direction, Ksi)	20.0
Shear Modulus (transverse ribbon direction, Ksi)	9.0

* Top or bottom sandwich facesheet thickness

Tank Structure Arrangements and Finite Element Models

The finite element model of the conformal tank with its internal structure is shown in Figure 2. Due to symmetry, only half of the tank structure is modeled. The 'exploded view' of the tank shown in Figure 3 includes the intertank, the LOX tank, the LH2 tank and other internal structures. The intertank is a structure that connects the liquid oxygen (LOX) and liquid hydrogen (LH2) cryogenic tanks. Internal structures maintain the tank shape and prevent large out-of-plane deformations. The three translational nodal displacements of the tank structure are fixed along the curve ABC near the rear end of its LH2 tank, and symmetry boundary conditions are applied on the symmetry plane (see Figure 2). The aforementioned "Maximum 3-G Axial Acceleration Load Condition" is applied to the tank structures. This loading condition consists of a transverse load (z-direction load) due to the angle-of-attack, axial load (x-direction load due to axial thrust and drag forces, tank ullage pressure, and tank hydrostatic pressure due to fluid under vehicle acceleration. The transverse and axial loads are applied to the tank outside surface as nodal forces. The ullage and hydrostatic pressures are applied as distributed pressures on the internal surfaces of the LOX and LH2 tanks.

All tank structures, including the walls of the LH2 and LOX tanks, intertanks, and tension ties are honeycomb sandwich constructions. Strength of materials formulae and the minimum gage requirements are used to set the upper and lower bounds of each design variable in the optimization analyses.

Cryogenic Tank Structure Optimization Analysis

The optimization problem is formulated as

Minimize weight $\quad min\ W(\bar{\mathbf{x}})$

Subject to constraints

LOX and LH2 Tank Walls:

strain

$-6{,}000 \le \text{Principal}\,\varepsilon(\bar{\mathbf{x}}) \le 6{,}000\ microstrain$

total facesheet thickness

$0.12\ in. \le TF(\bar{\mathbf{x}}) \le 0.25\ in.$

sandwich core thickness

$0.25\ in. \le TC(\bar{\mathbf{x}}) \le 3.0\ in.$

Intertank:

strain

$-6{,}000 \le \text{Principal}\,\varepsilon(\bar{\mathbf{x}}) \le 6{,}000\ microstrain$

total facesheet thickness

$0.12\ in. \le TF(\bar{\mathbf{x}}) \le 0.25\ in.$

sandwich core thickness

$0.25\ in. \le TC(\bar{\mathbf{x}}) \le 3.0\ in.$ *(Cylindrical regions)*

$0.6\ in. \le TC(\bar{\mathbf{x}}) \le 3.0\ in.$ *(Flat regions)*

Internal Structures:

strain

$-10{,}000 \le \text{Principal}\,\varepsilon(\bar{\mathbf{x}}) \le 10{,}000\ microstrain$

total facesheet thickness

$0.04\ in. \le TF(\bar{\mathbf{x}}) \le 0.25\ in.$

sandwich core thickness

$0.25\,in. \le TC(\bar{\mathbf{x}}) \le 3.0\,in.$

where $\bar{\mathbf{x}}$ represents the design variables.

The conformal tank structures are divided into 33 regions as shown in Figure 4. In each region, the composite facesheet and core thicknesses are treated as continuous variable. Since each region has two design variables, the total number of design variables for the conformal tank is 66. The lower bound of the core thickness of the intertank flat regions is set to 0.6 in. to ensure sufficient bending rigidity to prevent large out-of-plane deformation induced by the compression loads.

The structural optimization of the tank is performed using MSC/NASTRAN's optimization capability (solution sequence number SOL 200) [5]. To perform optimization analysis, a design model needs to be developed first whose essential features are the definition of design variables, the functional relations between these design variables and the structural sectional properties, the definition of the objective function, and the constraint bounds. Detailed MSC/NASTRAN input entries for setting a design model for honeycomb sandwich structures are presented in the Appendix. To test the completeness of the input entries and check the optimization analysis results, optimization analyses of a uniform cross-section beam and a three-section beam under a uniform distributed load are performed. These results are also presented in the Appendix.

MSC/NASTRAN incorporates three algorithms to perform structural optimization, including the Modified Method of Feasible Directions (MMFD) [7], Sequential Linear Programming (SLP), and Sequential Quadratic Programming (SQP) [2,3]. The Modified Method of Feasible Directions is used in most of the optimizations performed in this study. However, all three algorithms are gradient-based optimization procedures and can be trapped at a local minimum. Nongradient based algorithms such as Simulated Annealing [8] or Genetic Algorithms [9], that can prevent the optimizer from trapping at a local minimum, are not available in MSC/NASTRAN.

Technical Difficulties with Conformal Tank Optimization Analyses

Two optimization analyses are performed first, one starting from the upperbound of all design variables and one starting from the lowerbound of all design variables. Weight and maximum strain constraint violation vs. cycle number of these two optimization analyses are shown in Figures 5 and 6. The maximum strain constraint violation is defined as the maximum percentage of strain higher than the allowable strain. These figures show that optimization analyses can be used to reduce the weight of an overly conservative design or to modify an infeasible design to become a feasible design. The weight of an over-designed conformal tank is continuously reduced by the optimizer as shown in Figure 5. Furthermore, Figure 5 shows that there is no constraint violation at any part of the optimization cycle. Figure 6 shows that when starting from an infeasible design formed by the lowerbound of each design variable, weight is added during the initial cycles to create a feasible design. After the design becomes feasible, the optimizer then lowers the weight of the design.

The optimal designs obtained by using the upperbond and the lowerbound starting points are designated as Design A and Design B, respectively. The weight of Design A is and 53,983 lbs. and the weight of Design B is 36,283 lbs. as shown in Figures 5 and 6, respectively. The weight of Design A is about 50% heavier than the weight of Design B. A study to determine whether there are barriers that can prevent the optimizer moving from Design A to Design B is conducted.

In this study, a design line connecting the two optimal designs, Design A and Design B, is used. Nine intermediate points between the two end design points along the design line are created. If the vector of design variables of Design A is $\bar{x}_1$ and the vector of design variables of Design B is $\bar{x}_2$, the design points along the design line are

$$x = r \times \bar{x}_1 + (1-r) \times \bar{x}_2, \quad r = 0.0, 0.1, 0.2, 0.3, \ldots, 1.0 \qquad (1)$$

Linear static finite element analyses are performed to compute weight and evaluate constraint violation for each design point. It is found that weight is a linear function of r. However, some of the design points along the design line are infeasible designs, which violate strain constraints at r=0.7, 0.8 and 0.9 as shown in Figure 7. This indicates that the design space is nonconvex. Although the maximum strain constrain violation is less than 1.5%, this nonconvex design space can create local minima (barriers) to stop optimization analyses. For optimization solution convergence, the constraint violation tolerance limit is set to 0.5% as shown in Figure 7.

All strain constraint violations occur in an element that is located in the LOX tank rear dome (Design Region 5 in Figure 4) at the middle of the interface line among Design Regions 5, 6, and 10 (see Figures 4 and 8). The

strain change for this element as a function of r-value is plotted in Figure 8.

Optimization analyses using each design point along the design line as a starting point are also performed. Two optimization methods, the MMFD and the SLP, are applied. The optimal weights are plotted as a function of r-value as shown in Figure 9. Note that each method predicts a local minimum for each r-value. The local minimum weights for each r-value predicted by both methods agree very well with each other. A maximum difference of about five percent occurs at r=0.6. For this tank design there appears to be many local minima. A simple procedure that can create a better starting point for the optimizer is presented in the following section.

An Improved Optimization Procedure for Weight Reduction

In this procedure, a new starting point is assembled by selecting the lowest design value for each design variable in any of the aforementioned eleven optimal designs obtained by the MMFD. An additional optimization analysis is then performed using this new vector of design variables as a starting point. The new optimal design (Design C) has weight of 35,533 lbs. which is 750 lbs. lower than the previous lowest weight design (Design B). No further weight reductions of significance are found by searching in the vicinity of Design C. Furthermore, a few additional optimization analyses using various selected starting points that are not on the design line are conducted. Optimal weights from these analyses are all higher than the weight of Design C.

The design values and strain distributions of each region of the final design are then examined. It is found that high local strains dictate the design of Design Region 21 in Figure 4. Thus, it is expected that splitting the high strain elements out to form an additional design region may achieve further weight reduction. The high stress areas at two corners of Design Region 21 are isolated to form a new design region. Thus, the Design Region 21 is split into Design Regions 21a and 21b as shown in Figure 10. An optimization analysis is performed with this modified model and a final design with a weight of 34,492 lbs is obtained. The design variable values and analysis results of this configuration are reported in the following sections.

Thicknesses and Weights of Tank Structures

The sandwich facesheet thickness, core thicknesses, and weight of each design region are listed in Table 3. Most of the sandwich tank wall facesheets are at the minimum gage thickness. The distributions of total facesheet thickness and core depth of the final sandwiched conformal tank walls are plotted in Figures 11 and 12, respectively.

Table 3. Design variable values and weight.

Design Region	Total Facesheet Thickness (in.)	Core Thickness (in.)	Weight (lbs.)
1	0.12	0.25	935
2	0.12	0.25	681
3	0.12	0.28	687
4	0.17	0.66	1283
5	0.19	0.45	1489
6	0.23	0.34	844
7	0.12	0.25	33
8	0.12	0.26	98
9	0.15	0.76	226
10	0.04	0.28	579
11	0.04	0.28	501
12	0.04	0.28	282
13	0.04	0.27	100
14	0.04	0.27	100
15	0.12	1.30	1189
16	0.12	0.30	2169
17	0.12	0.28	945
18	0.12	0.34	1047
19	0.12	0.82	1164
20	0.15	1.63	1940
21a	0.15	0.29	1060
21b	0.25	1.54	83
22	0.12	0.31	1099
23	0.15	0.61	902
24	0.12	0.44	867
25	0.14	2.83	1695
26	0.25	3.00	4288
27	0.04	1.70	1213
28	0.09	0.51	1561
29	0.09	0.79	351
30	0.06	0.27	2424
31	0.04	1.61	876
32	0.04	0.26	884
33	0.04	0.26	897

Total Weight: 34,492 lbs.

The weight breakdown of the five major components of the final design is shown in Figure 13. Note that a significant portion of the weight, about 29% of the conformal tank weight, is due to LOX and LH2 tank internal structures. Therefore, potential further weight reduction may be achieved by changing the design of the internal structures.

Linear and Nonlinear Structural Analysis Results

The MSC/NASTRAN design optimization procedure computes design sensitivities based on linear static finite element analysis results. Geometrically nonlinear effects are not considered. Thus, geometrically nonlinear analyses need to be performed to confirm that the final tank structure can meet the design requirements. If the nonlinear analysis results indicate some regions violate the design requirements, these regions need to be resized.

Nonlinear analyses of the final design of the conformal tank are performed. An initial nonlinear analysis reveals that a deformation larger than that expected occurs in the flat portions of the intertank; thus the core thickness of the intertank is increased to 2.5 inches. A linear analysis and a nonlinear analysis are performed for comparison. Plots of major principal strains of the outside LOX and LH2 tank walls obtained from both analyses are shown in Figures 14 and 15. These results show that the final LOX and LH2 tank-wall designs for the conformal tank can meet the design strain allowable of 6,000 microstrain. The nonlinear membrane stress stiffening effect lowers the strains in the flat regions of the conformal LOX tank and the rear cylindrical region of the conformal LH2 tank.

Further Design Improvement Areas

This study used structural optimization to conduct sizing of tank structures in the early design stage. Similar optimization procedures can be used in the detailed design stage of the tank structures. The following three design approaches are recommended for further weight reduction.

1. Local high stress concentration areas within a particular design region will dictate the sandwich facesheet and core thicknesses for the entire design region. If a design region is separated into a low stress design region and a high stress design region, significant weight reduction from the low stress region is possible. Note that this approach is used to reduce the weight of Design Region 21.
2. More cutouts can be added to the LOX and LH2 internal structures. In this study only the Design Regions 12 and 30 have cutouts.
3. The nonlinear membrane stiffening effect is expected to reduce the bending deformation in some tank regions. Using nonlinear analyses instead of linear analyses in the optimization process may achieve a lower weight design.

Concluding Remarks

The structural optimization analysis capabilities in MSC/NASTRAN were used to size a conformal cryogenic tank's honeycomb sandwich structures. This tank is divided into 33 design regions. The facesheet thickness and the honeycomb core depth of each design region are the design variables. The MSC/NASTRAN input entries for setting the design model to optimizing these design variables for a minimal weight tank design were developed.

This study found that the feasible design space for this problem is nonconvex and many local minima are exhibited. Because MSC/NASTRAN does not guarantee to find the global minimum, a simple procedure, which has potential to create a better starting point for the optimizer, was introduced. This procedure was used to obtain a final improved lightweight design. Geometrical nonlinear analysis results confirmed that this final LOX and LH2 tank-wall designs meet the strain constraints. Finally, areas that could have potential for further weight reductions were discussed.

References

1. Vanderplaats, G. N., *Numerical Optimization Techniques for Engineering Design with Applications*, McGraw Hill, 1984.
2. Arora, J. S., *Introduction to Optimum Design*, McGraw Hill, 1989.
3. Haftka, R. T. and Gurdal, Z, *Elements of Structural Optimization*, Kluwer Academic Publishers, 1992.
4. Dorsey, J. T., Myers D. E. and Martin, C. J., Jr., Reusable Launch Vehicle Tank/Intertank Sizing Trade Study, 38th AIAA Aerospace Sciences Meeting and Exhibit, Reno, Nevada, AIAA 2000-1043, January 10-13, 2000.
5. Moore, G. J., *MSC/NASTRAN Design Sensitivity and Optimization User's Guide*, V67, 1993.
6. Dorsey, J. T., Wu, K. C., Rivers, H. K., Martin, C. J., Jr. and Smith R. W., Airframe Integration Trade Studies for a Reusable Launch Vehicle, Space Technology and Applications International Forum (STAIF '99), Albuquerque, New Mexico, January 31-February 4, 1999.
7. Vanderplaats G. N., "An Efficient Feasible Directions Algorithm for Design Synthesis," AIAA Journal, Vol. 22, NO. 11, pp. 1633-1640, November 1984.
8. Laarhoven,P.J.M. van., and Aarts, E., *Simulated Annealing: Theory and Applications*, D. Reidel Publishing, Dordrecht, The Netherlands, 1987.
9. Goldberg, D. E., *Genetic Algorithms in Search, Optimization, and Machine Learning*, Addison-

Wesley Publishing Co. Inc., Reading, Massachusetts, 1989.
10. MSC/NASTRAN Quick Reference Guide, Version 70.5, The MacNeal-Schwendler Corporation, 1998.

Acknowledgements

The authors would like to acknowledge Dr. C. Kim of Eagle Aeronautics, Inc. for creating the finite element models. The suggestion of conducting a design line study by Professor Raphael T. Haftka of University of Florida is highly appreciated.

Appendix

Design Model for Sandwich Structure Optimization

MSC/NASTRAN SOL200 input entries to build a design model for optimizing sandwich structures are developed. A sandwich beam shown in Figure A-1 is analyzed to test the completeness of these input entries and verify the results. The beam is 30 inches long and is subjected to a uniformly distributed load of 100 lbs/in. The beam is divided into three different sections. Two different optimization analyses are performed: the first consists of a uniform beam which has the same facesheet and core thicknesses for all three sections and the second consists of a three-section beam in which each section has different facesheets and core thicknesses. The material properties listed in Table 1 are used.

The optimization statements are:

Minimize weight $\quad min\ W(\bar{x})$

Subject to constraints:

strain

$-1000 \le Axial\ \varepsilon(\bar{x}) \le 1{,}000\ microstrain$

total facesheet

$0.12\ in. \le TF(\bar{x}) \le 0.24\ in.$

sandwich core

$0.1\ in. \le TC(\bar{x}) \le 4.0\ in.$

where $\bar{x}$ are design variables.

The key inputs include the design variables (DESVARs), design equations (DEQATNs), design variable to analysis property relations (DVPREL1), design variable to analysis property relations using user-supplied DEQATNs (DVPREL2), design sensitivity response quantities (DRESP1), design constraints (DSCONs) and design optimization parameters (DOPTPRM).

The DEQATNs inputs related to MSC/NASTRAN's PSHELL data entry [10] are

```
DEQATN 101   NSM(TF,TC) = TC*RHO
DEQATN 201   Z1(TF,TC) = -0.5*(TC+TF)
DEQATN 301   Z2(TF,TC) = 0.5*(TC+TF)
DEQATN 401   ST(TF,TC) = TC/TF
DEQATN 501   BI(TF,TC) =
             3.0*(TC/TF+0.5)**2+0.25
```

where *TF* is the total facesheet thickness (top and bottom facesheets),
TC is the core thickness,
RHO is the core density,
NSM is the honeycomb core areal density,
Z1 and *Z2* are the fiber distances from the reference surface,
ST is the transverse shear thickness ratio (transverse shear uniformly carried by the core only),
and *BI* is the bending moment initial ratio:

$$BI = \frac{12 \times I}{TF^3} \qquad \text{(A-1)}$$

where the bending rigidity (I) of the beam can be expressed as

$$I = \frac{(TF)^3}{48} + \frac{TF\left(TC + \frac{TF}{2}\right)^2}{4} \qquad \text{(A-2)}$$

The DVPREL1 and DVPREL2 inputs are created based on the MSC/NASTRAN's shell element property (PSHELL) format using DESVARs and DEQATNs.

The DRESP1 entries define a set of structural responses that are used in the design either as constraints or as an objective. The DSCONS entries define design constraints in design sensitivity analysis. The DOPTPRM entries are used to override default values of parameters used in design optimization.

Beam Results

The optimized uniform cross-section beam has a facesheet thickness of 0.159 in. and a core thickness of 3.047 inches. In the optimized 3-section beam, Sections 1 and 3 have the same facesheet thickness of 0.146 in. and same core thickness of 2.742 in; and Section 2 has a facesheet thickness of 0.153 in. and a core thickness of 3.173 in. The weight for the uniform cross-section beam and the three-section beam are 0.408 and 0.383 lbs, respectively.

The top-surface axial strain plots of the uniform beam and the 3-section beam are shown in Figure A-2. The strain results of the uniform beam agree with the closed form solutions. The 3-section beam has a much longer section subjected to a high strain near the maximum strain of 1,000 microstrain as expected.

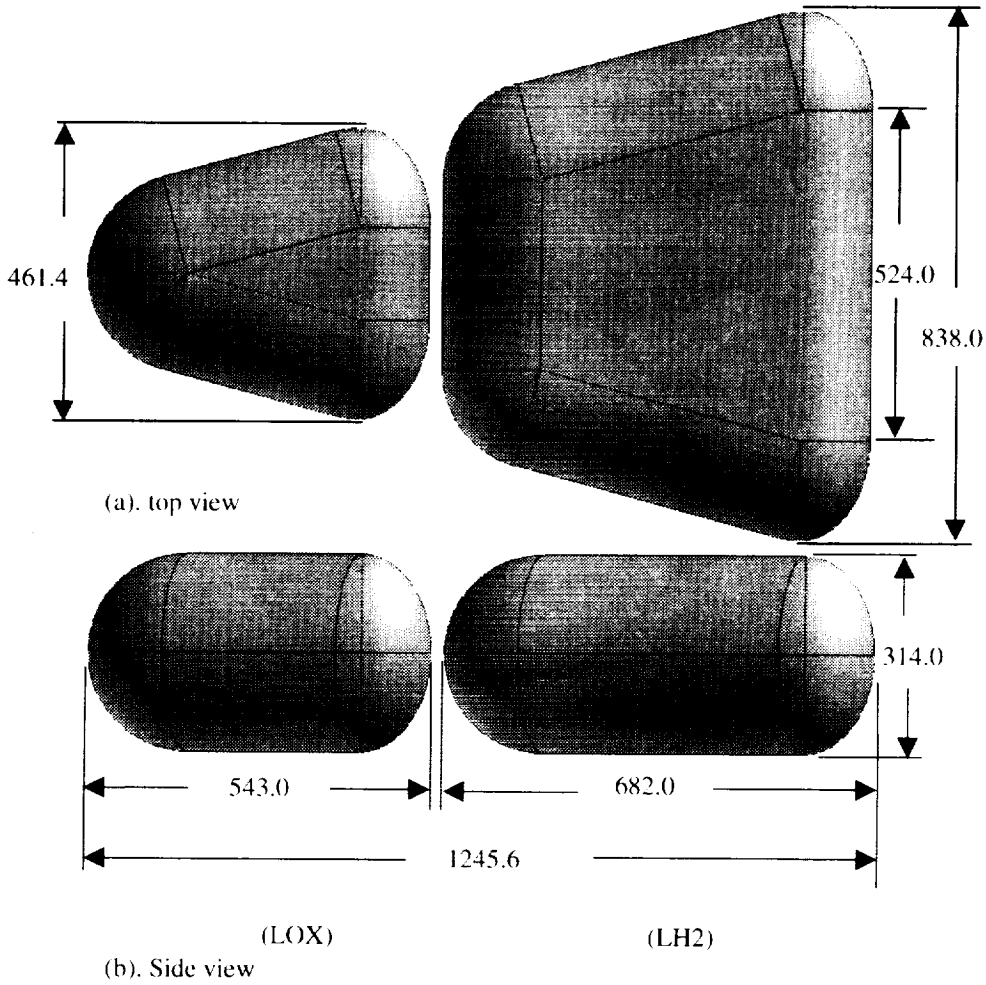

Figure 1. Dimensions of conformal tanks (in.).

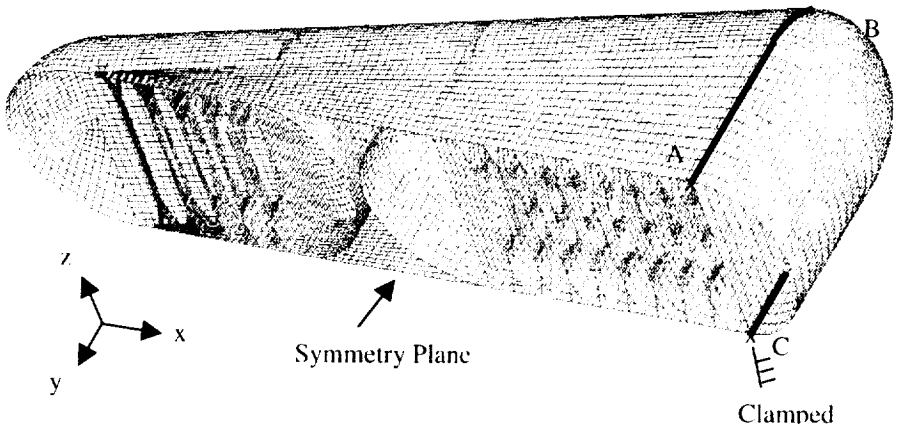

Figure 2. Finite element model of a symmetric half of the conformal tank.

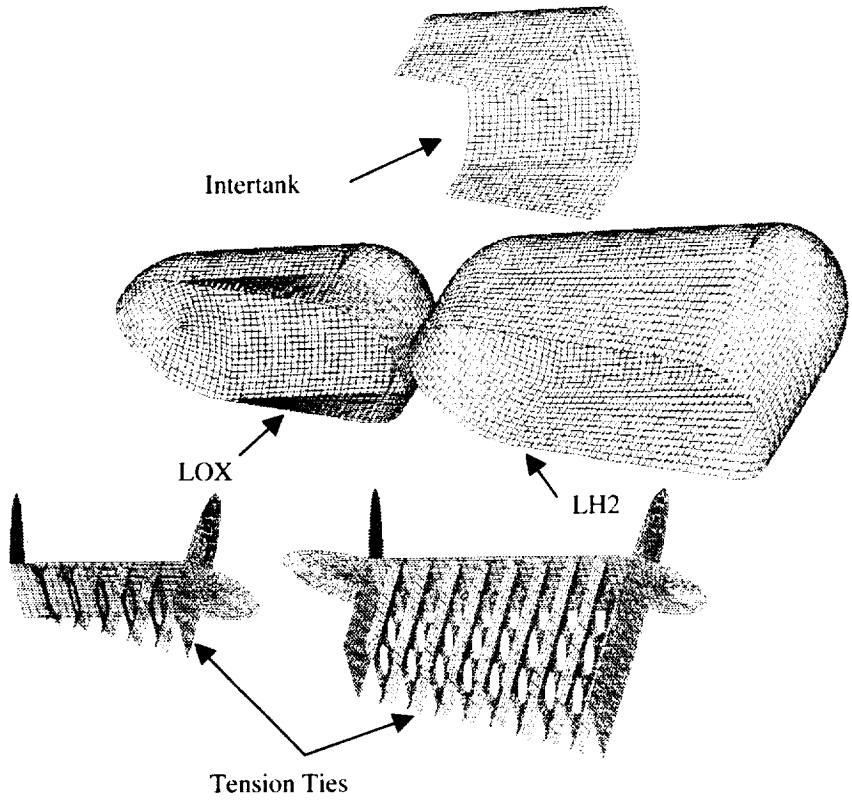

Figure 3. Substructures of conformal tank configuration.

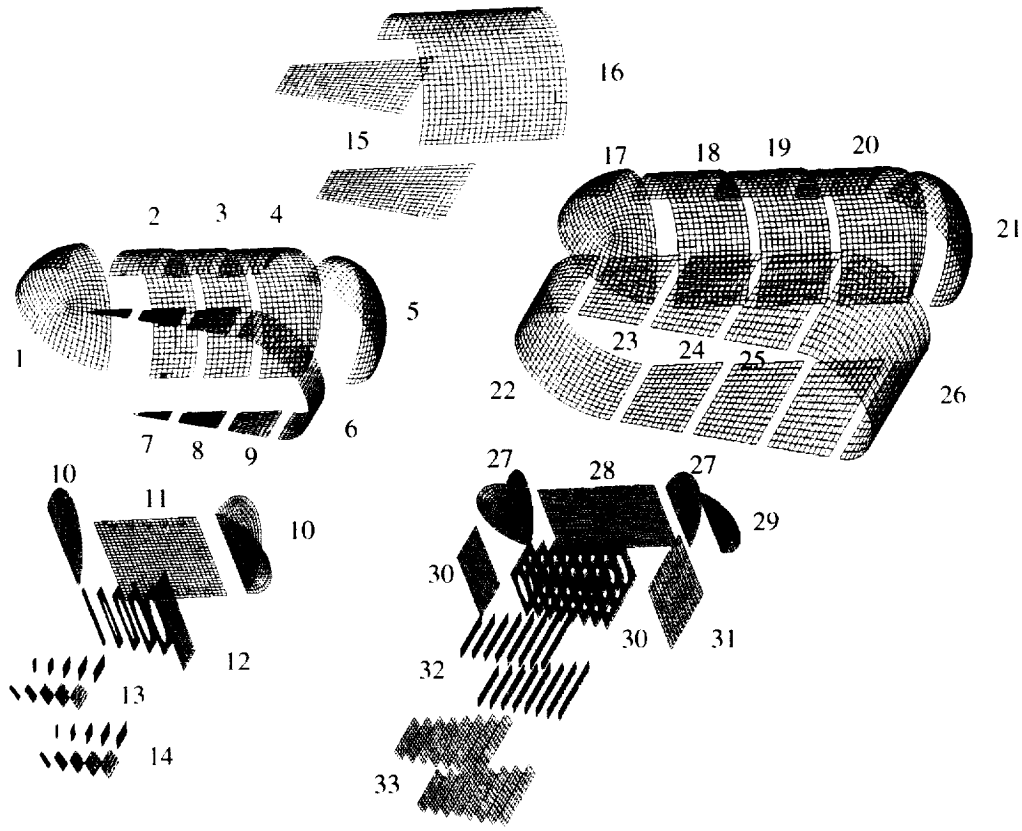

Figure 4. Design regions.

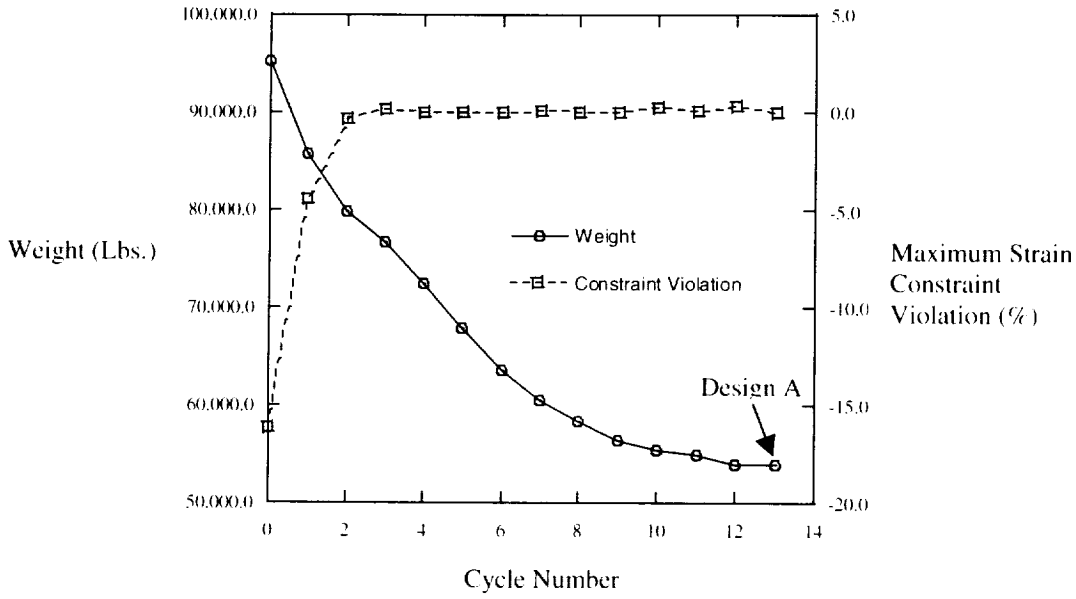

Figure 5. Optimization analysis starting from the upperbound of all design variables.

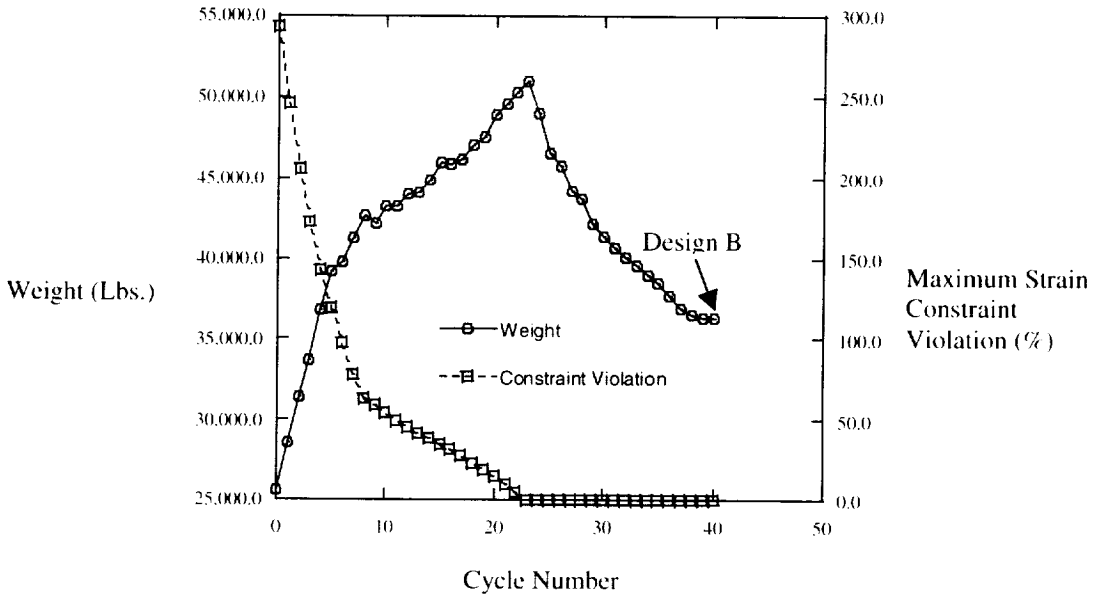

Figure 6. Optimization analysis starting from the lowerbound of all design variables.

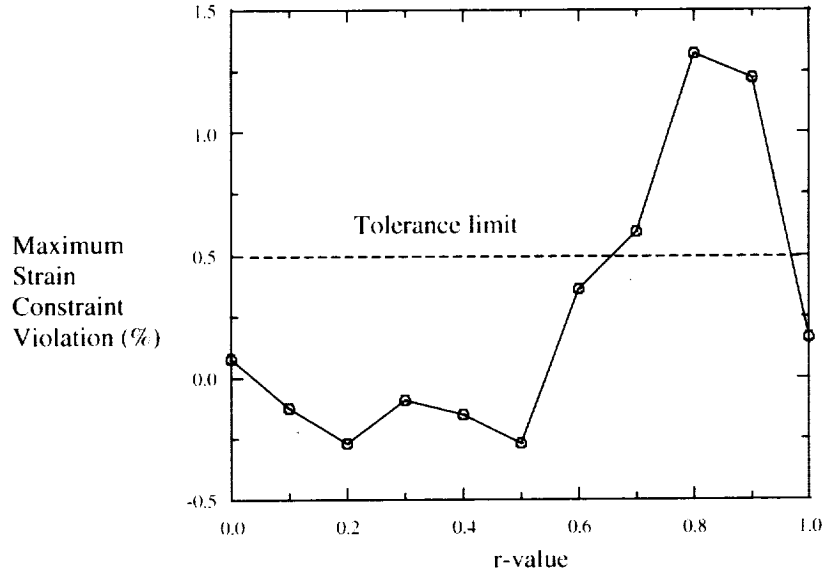

Figure 7. Infeasible design at r=0.7, 0.8, and 0.9.

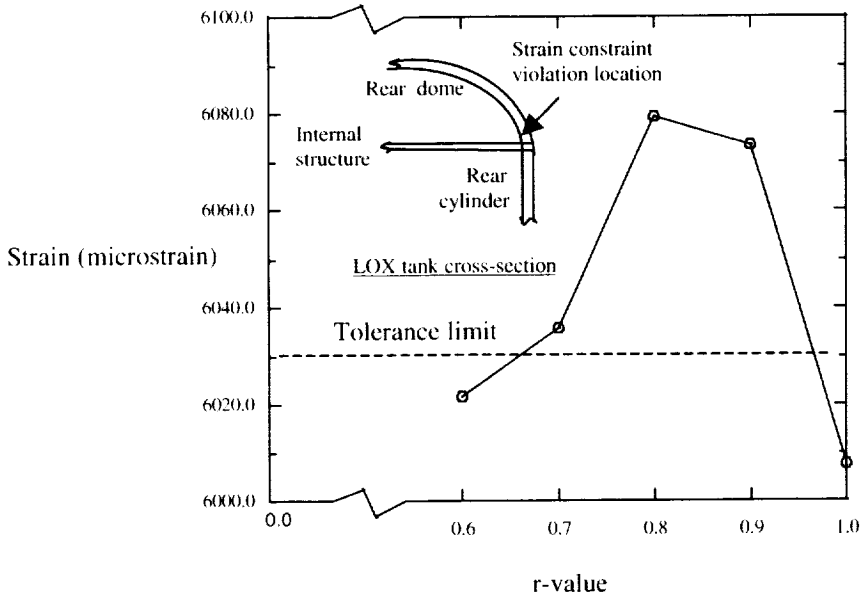

Figure 8. Strain changes as a function of r-value at the constraint violation location.

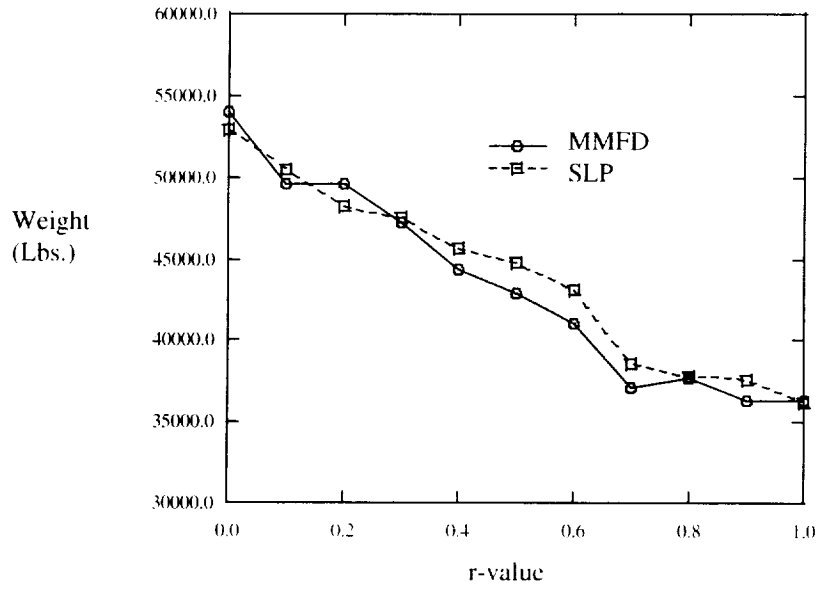

Figure 9. Weight vs. r-value plot for MMFD and SLP methods.

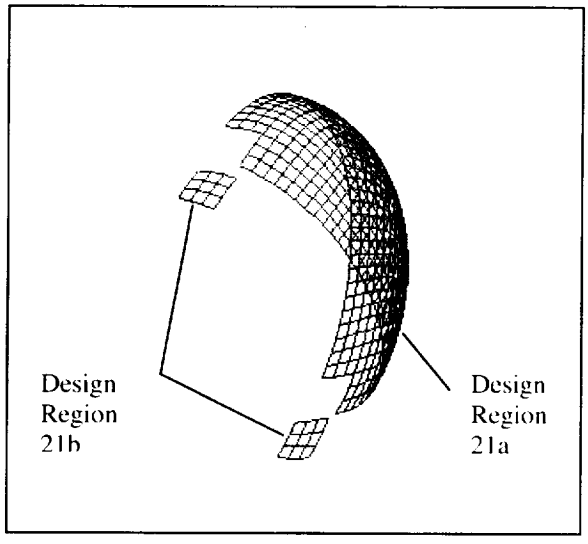

Figure 10. Design Region 21 separated into a low stress region (21a) and a high stress region (21b).

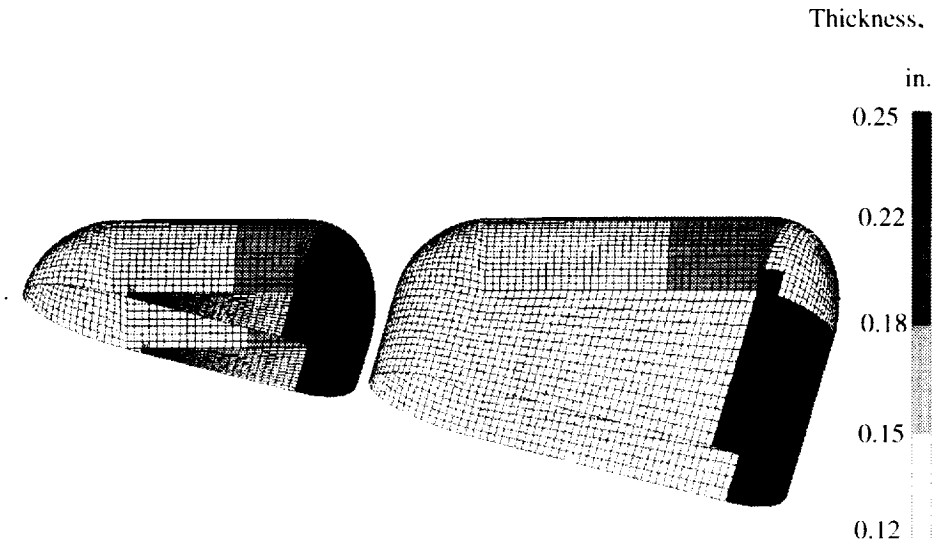

Figure 11. Total facesheet thickness distribution of the conformal LOX and LH2 tanks.

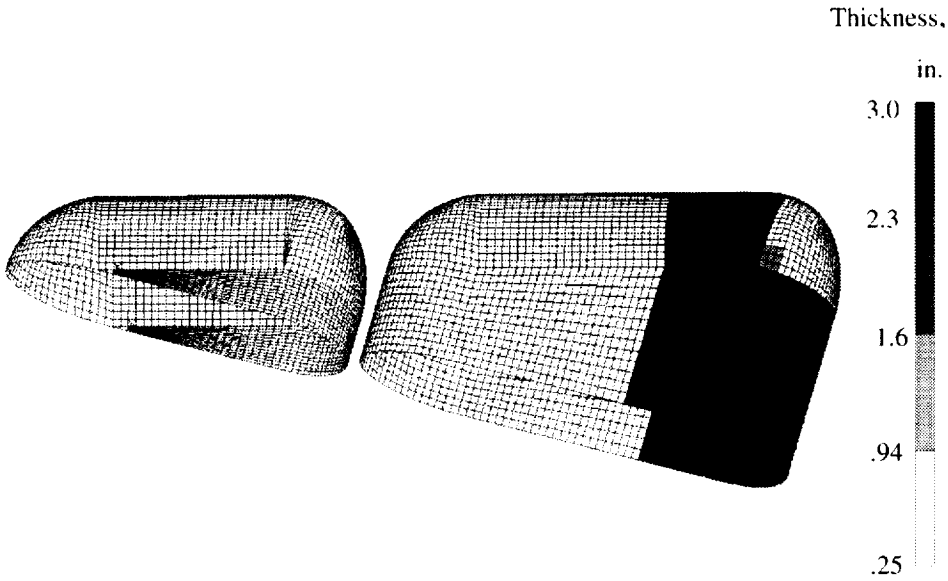

Figure 12. The core depth distribution of the conformal LOX and LH2 tanks.

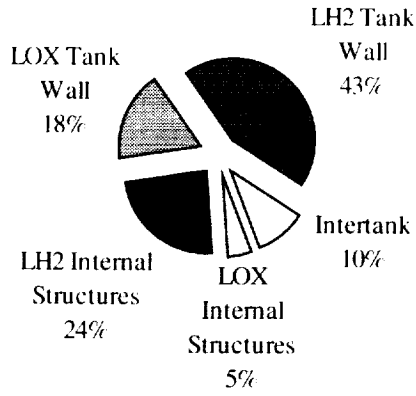

Figure 13. Weight distributions of major tank substructures.

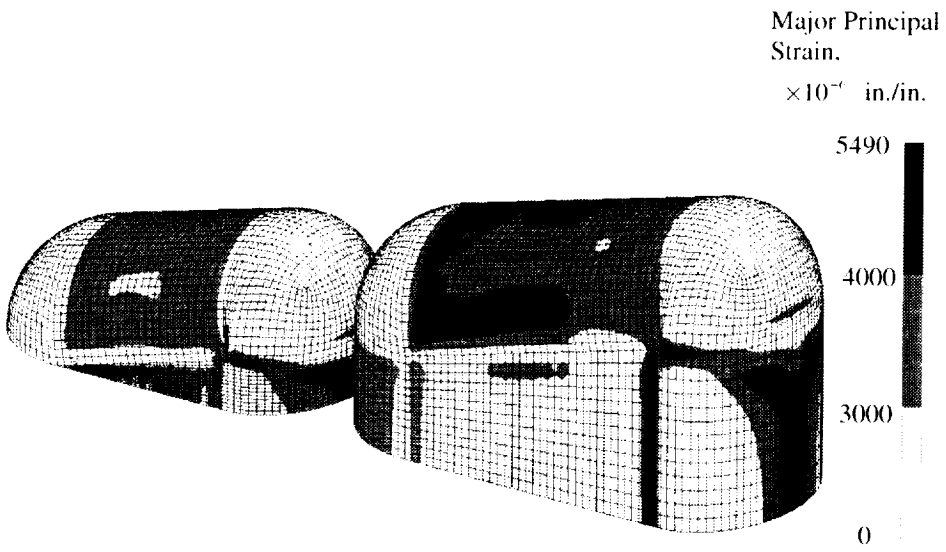

Figure 14. Strain plot of conformal tank from linear analysis.

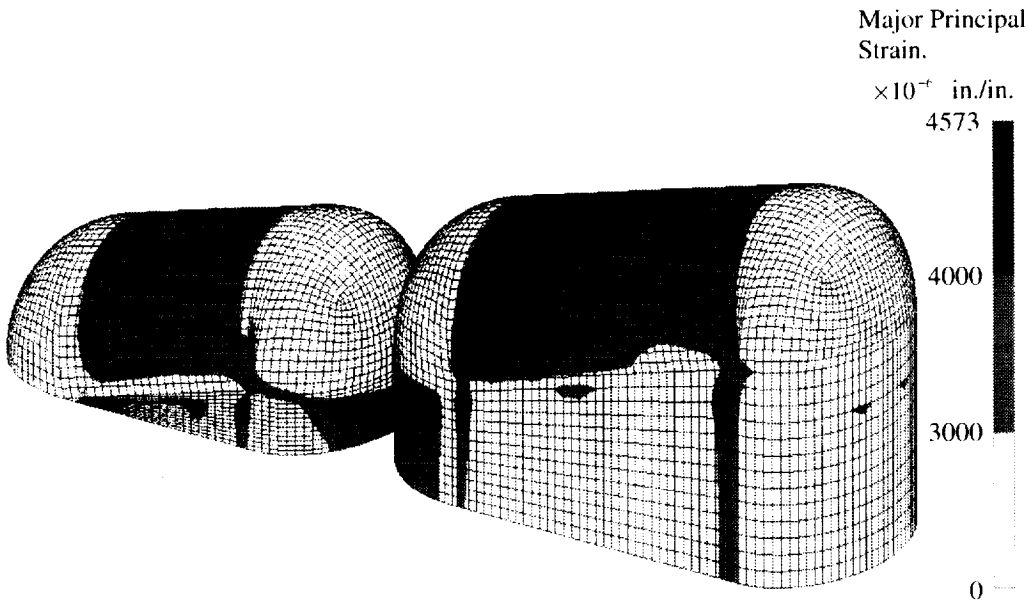

Figure 15. Strain plot of conformal tank from nonlinear analysis.

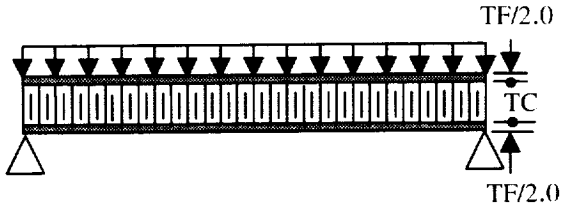

Figure A-1. Beam under a uniform distributed load.

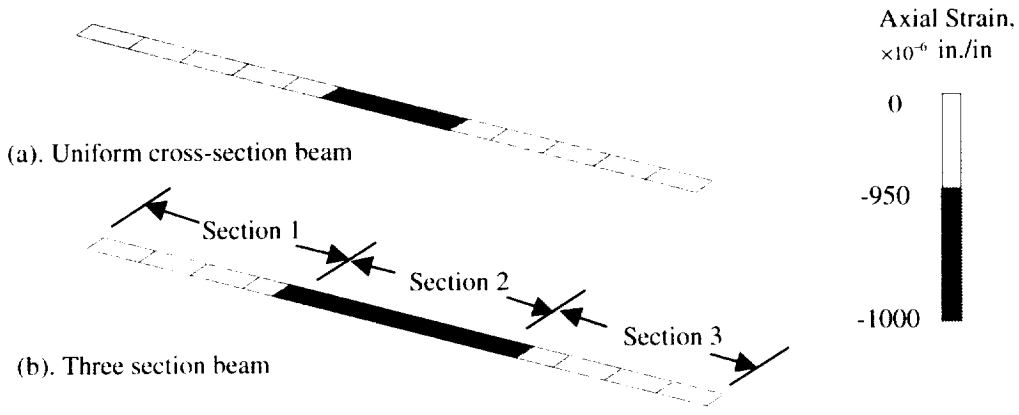

Figure A-2. Axial strain plot for the beam top surface.